Brain Stimulation 12 (2019) 724–734

Contents lists available at ScienceDirect

Brain Stimulation

journal homepage: http://www.journals.elsevier.com/brain-stimulation

Personalized striatal targets for deep brain stimulation in obsessive-compulsive disorder

Juan A. Barcia [a, b, *], Josué M. Avecillas-Chasín [a], Cristina Nombela [a], Rocío Arza [a], Julia García-Albea [c], José A. Pineda-Pardo [d], Blanca Reneses [c], Bryan A. Strange [e, f]

[a] Service of Neurosurgery, Hospital Clinico San Carlos, Instituto de Investigación Sanitaria del Hospital Clínico San Carlos, Madrid, Spain
[b] Department of Surgery, Universidad Complutense de Madrid, Madrid, Spain
[c] Service of Psychiatry, Hospital Clinico San Carlos, Instituto de Investigación Sanitaria del Hospital Clínico San Carlos, Madrid, Spain
[d] CINAC, HM Puerta del Sur, Hospitales de Madrid, Mostoles, and CEU-San Pablo University, Madrid, Spain
[e] Laboratory for Clinical Neuroscience, Centre for Biomedical Technology, Universidad Politecnica de Madrid, Spain
[f] Department of Neuroimaging, Reina Sofia Centre for Alzheimer's Disease, Madrid, Spain

ARTICLE INFO

Article history:
Received 13 March 2018
Received in revised form
5 December 2018
Accepted 15 December 2018
Available online 20 December 2018

Keywords:
Deep brain stimulation
Striatum
Obsessive-compulsive disorder
Functional MRI
Probabilistic tractography

ABSTRACT

Background: Psychiatric conditions currently treated with deep brain stimulation (DBS), such as obsessive-compulsive disorder (OCD), are heterogeneous diseases with different symptomatic dimensions, indicating that fixed neuroanatomical DBS targets for all OCD cases may not be efficacious.
Objective/hypothesis: We tested whether the optimal DBS target for OCD is fixed for all patients or whether it is individualized and related to each patient's symptomatic content. Further, we explored if the optimal target can be predicted by combining functional neuroimaging and structural connectivity.
Methods: In a prospective, randomized, double-blinded study in 7 OCD patients, symptomatic content was characterized pre-operatively by clinical interview and OCD symptom-provocation during functional MRI. DBS electrode implantation followed a trajectory placing 4 contacts along a striatal axis (nucleus accumbens to caudate). Patients underwent three-month stimulation periods for each contact (and sham), followed by clinical evaluation. Probabilistic tractography, applied to diffusion-weighted images acquired pre-operatively, was used to study the overlap between projections from the prefrontal areas activated during symptom provocation and the volume of activated tissue of each electrode contact.
Results: Six patients were classified responders, with median symptomatic reduction of 50% achieved from each patient's best contact. This was located at the caudate in 4 cases and at the accumbens in 2. Critically, the anatomical locus of the best contact (accumbens or caudate) was related to an index derived by combining functional MRI responses to prevailing symptom provocation and prefronto-cortico-striatal projections defined by probabilistic tractography.
Conclusion: Our results therefore represent a step towards personalized, content-specific DBS targets for OCD.

Introduction

Following the success of deep brain stimulation (DBS) in treating certain neurological conditions such as Parkinson's disease and essential tremor, DBS is being increasingly used in the management of psychiatric disorders, including treatment-resistant obsessive-compulsive disorder (OCD) [1–4]. OCD is characterized by intrusive distressing thoughts (obsessions) and/or repetitive mental or behavioral acts (compulsions) and is a leading cause of illness-related disability [5,6]. DBS for OCD has targeted regions considered components of the reward and motivation system, such as the nucleus accumbens (NAcc) [7], the ventral capsule/ventral striatum VC/VS [8] and the limbic portion of the subthalamic nucleus (STN) [9], as well as the anterior limb of the internal capsule (ALIC) [10] and the inferior thalamic peduncle (ITP) [11]. One fundamental limitation, however, is that, in contrast to neurological conditions such as essential tremor where the symptomatology is relatively fixed across patients, psychiatric symptoms show heterogeneity in

* Corresponding author. Service of Neurosurgery, Hospital Clinico San Carlos, C/ Prof. Martín Lagos, s/n, 28040, Madrid, Spain.
E-mail address: jabarcia@ucm.es (J.A. Barcia).

https://doi.org/10.1016/j.brs.2018.12.226
1935-861X/

terms of their content. In treatment-resistant OCD patients undergoing DBS this is particularly relevant. OCD is a heterogeneous disease in which different behaviors, or symptomatic dimensions, are expressed [12]. Patients may show obsessions or compulsions of contamination and washing, forbidden thoughts, doubts and checking, symmetry and ordering, repeating or hoarding [13]. Seventy-four percent of patients are reported to fit into this classification [14], and some patients express a combination of symptom dimensions. Despite this heterogeneity, current DBS approaches target the same site across patients, regardless of the content of their symptoms.

Determining the predominant symptoms in a given patient relies on clinical evaluation. The characterization of the neural substrates of different symptomatic dimensions in OCD has employed functional magnetic resonance imaging (fMRI), applied in the context of presenting patients with images corresponding to specific symptom dimensions using the Maudsley Obsessive-Compulsive Stimuli Set (MOCSS) [15]. This symptom provocation method reveals activations in different areas of the prefrontal cortex, selectively for each symptomatic dimension. For example, patients with contamination obsessions mainly activate the medial orbitofrontal (ventromedial) cortex, while those who present checking symptoms chiefly activate the dorsolateral prefrontal cortex (PFC) [15]. These different areas of the prefrontal cortex project to the striatum into different ventrodorsally distributed areas, and not only to the NAcc or ventral striatum (VS). For example, ventromedial and orbitofrontal cortex project to NAcc, but dorsal anterior cingulate and dorsolateral PFC project to more dorsal portions of the striatum [16–18]. Given that the pathophysiology of obsessive-compulsive disorder (OCD) is thought to involve abnormal activity in fronto-striatal circuits [19,20], differential engagement of PFC subdivisions during the MOCSS task as a function of symptom dimension is important because it implies that different subdivisions of the striatum may be differentially implicated in a given OCD patient's pathophysiology. Thus, if during symptom provocation a patient exhibits increased activity in dorsal frontal areas, which form part of fronto-striatal circuits involving striatal regions dorsal to the NAcc, it is possible that this patient will not improve with NAcc or VS stimulation simply because DBS has not targeted the pathological circuit.

Recent studies on DBS in OCD have shown that the overall control achieved by stimulating different targets (the same single target being used in all patients within each cohort) is about 50% of clinical responders [21,22]. This contrasts with patients with essential tremor, in whom thalamic DBS produces postural tremor reduction in 89% of cases [23]. We considered that the explanation for the 50% clinical response rate is the approach of treating all OCD cases with a single target, independently of their symptom content. We hypothesized that the optimal striatal target for DBS in OCD patients is located along the dorsoventral axis of the striatum – not limited to the NAcc (or VS) – depending on the dysfunctional fronto-striatal circuit. This, in turn, would depend on the particular symptom dimension of each patient, with predominant symptom(s) defined as the most severe, resistant to treatment and disabling OCD symptoms at the time of recruitment. To test this hypothesis, we characterized symptom content-specificity of individual OCD patients using symptom-provocation fMRI prior to DBS implantation. Subsequently, in a prospective double-blinded study in a series of 7 OCD patients that were candidates for psychiatric surgery, we tested the clinical efficacy of different electrode contacts distributed along the striatum, spanning the caudate and NAcc (Fig. 1). This comprised three months of bilateral stimulation (4.5 V stimulation at a frequency of 130 Hz and pulse-width 60 μs) in every electrode contact (0, 1, 2, 3) and sham period (no stimulation). Furthermore, we present a novel method to determine, *a priori*, which stimulation site would be optimal. Patients underwent pre-operative diffusion-weighted MRI imaging (DWI) and projections between prefrontal activations during symptom provocation and the 4 contact points along the striatal axis were determined by applying probabilistic tractography to these images. For each stimulated site, the density of prefronto-striatal projections was subsequently compared with clinical efficacy of stimulation.

Methods

Patients

Seven patients, three male aged 21–50 years; average 36.67, and four female aged 28–46 years; average 35.25, suffering from treatment-refractory obsessive-compulsive disorder participated in this study. All patients scored 24 or higher in the Yale-Brown Obsessive- Compulsive Scale (Y-BOCS) [24]. All patients provided written informed consent. The study had approval from the Hospital Clínico San Carlos Ethics Committee. The study is registered at clinicaltrials.gov under trial name "Deep brain Stimulation in Obsessive-compulsive Disorder: Randomized, Double-blinded Clinical Trial (10/131)", registration number: NCT03217123.

Patient inclusion

Between June 2011 and December 2014, all patients diagnosed with OCD who attended the outpatient clinic at the Psychiatry Department of Hospital Clínico San Carlos (Madrid, Spain) and met study inclusion criteria were invited to participate in this study. Patient demographic details are provided in Table S1. Inclusion criteria for functional neurosurgical management were a) age 18–50 years; b) severe chronic form of treatment-resistant OCD according to DSM-IV Revised criteria; c) duration of illness of at least 5 years without remission; d) a Y-BOCS score $\geq$24/40; e) treatments with maximum tolerated dose of at least five serotonin reuptake inhibitors for at least 10 weeks, treatment with clorimipramine, buspirone and lithium for at least 4 weeks, as well as psychotherapy (a minimum of 20 sessions of therapist-guided exposure and response prevention) simultaneously with pharmacotherapy; f) no changes in prescribed medication for at least 4 weeks before; g) inability to carry out a normal social/family life and impairment in daily life function; h) availability of protective and supportive legal, social and familial environment for surgical treatment and rehabilitation periods; i) consensus that the patient is a candidate for DBS for OCD by two independent psychiatrists, with approval from an independent psychiatric surgery committee composed of one neurosurgeon, one psychiatrist and one legal medicine expert; j) ability to provide written consent for the study.

Exclusion criteria were: a) past or present diagnosis of psychotic disorder; b) present or past substance abuse; c) any current clinically significant neurological disorder or medical illness; d) any clinically significant abnormality on preoperative magnetic resonance imaging; e) any DBS contraindication.

All patients were blind to stimulation protocol throughout the study.

Psychiatric assessment

Y-BOCS was the primary psychiatric variable for this study. Predominant obsessions and compulsions for each patient were recorded at baseline according to standardized evaluation using Y-BOCS total score. Additionally, clinical change was measured by the Global Assessment of Function (GAF) score [25] and the Clinical Global Impression (CGI) [26]. Thus, patients were clinically assessed with Y-BOCS, GAF and CGI at baseline, at the end of every trial –

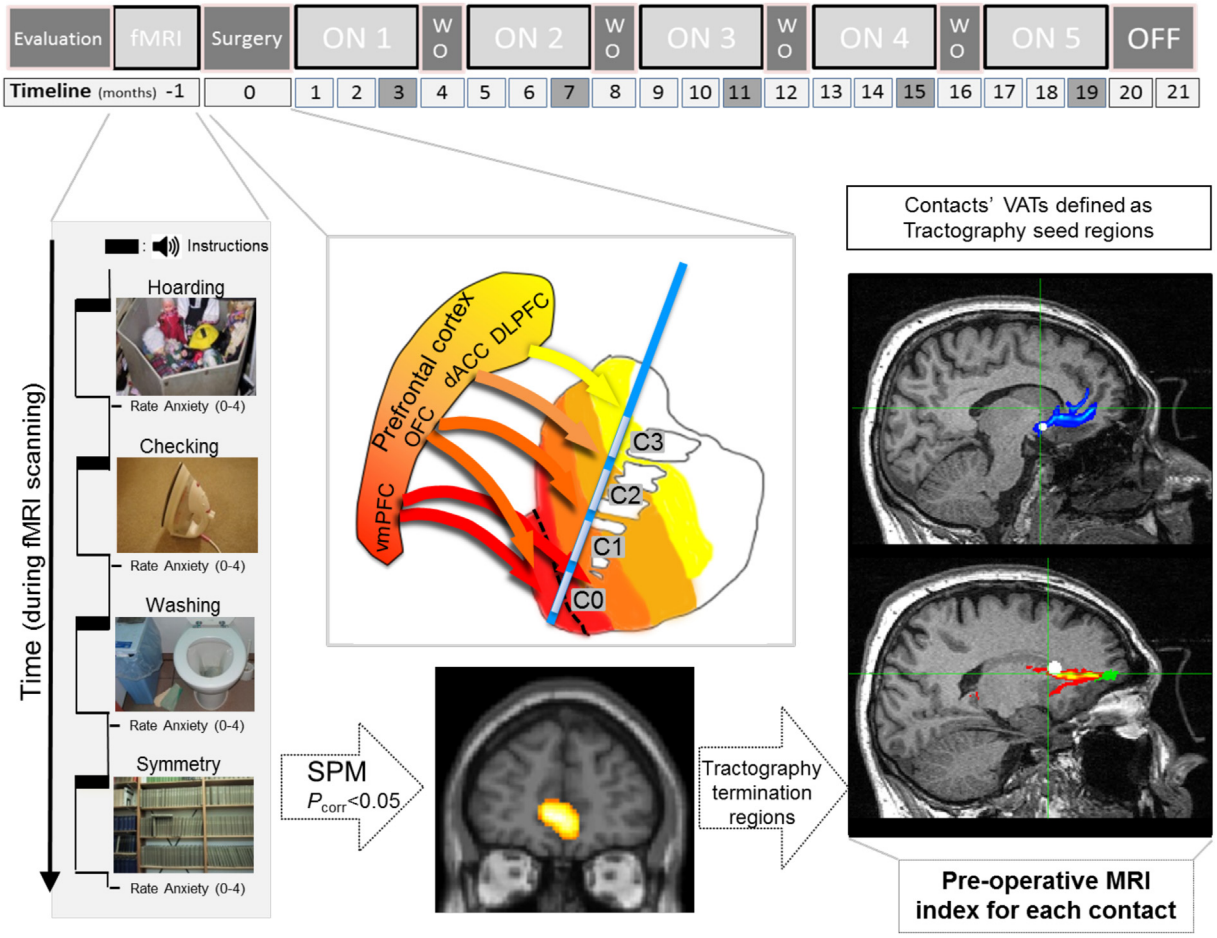

Fig. 1. Study design. The study timeline (top) indicates the phases of the study and the duration of each phase in months. During surgery, bilateral deep brain stimulation electrodes with four contact (C0 to C3) were place along the striatum (centre). Time 0 is defined as the beginning of the first ON trial of stimulation (**ON 1**). Each trial lasted 3 months and was followed by a one month washout (**WO**) period. Note that there are 5 ON trials, which pertain to the 4 electrode contacts and one sham trial. The pre-operative phase consisted of psychiatric and neuropsychological evaluation, followed by a symptom provocation study in the context of functional magnetic resonance imaging (fMRI; below left). fMRI data were analyzed to define patient-specific responses to predominant symptoms provocation (below middle). The thresholded activations were defined as termination regions during a probabilistic tractography analysis (below right), which used volume of activated tissue (VAT) around each contact as seeds. The striatum schema was taken from Haber and Knutson, 2009 [17] (Haber SN, Knutson B. The Reward Circuit: Linking Primate Anatomy and Human Imaging. Neuropsychopharmacology 2009;35:4–26). Permission requested.

three months of stimulation in every contact: 0, 1, 2, 3 and sham period – and after each one-month wash-out period. Standardized clinical evaluation was done by a psychiatrist who was blind to stimulation protocol. Pharmacological treatment did not change during the study period in all cases with the exception of small variations in benzodiazepine dosage. Psychiatric scores along all trials are provided in Table S2.

Neuropsychological assessment

Neuropsychological evaluation was conducted following each psychiatric assessment, with evaluator blind to stimulation protocol. The main cognitive domains were assessed: Free Cued Serial Recall Test [27] in abbreviated form (only 2 of the 3 test trials) for learning and memory (3 different versions of the task were used across the longitudinal study); Stroop Color-Word Interference Test [28] for cognitive control and inhibition; phonological verbal fluency [29] and categorical verbal fluency [30] for verbal fluency [31]; Letter-number sequencing from WAIS-IV for Working memory [32]; Trail Making test subtest A (TMT-A) and subtest B (TMT-B) [33] for sustained and divided attention, and the Wisconsin Card Sorting Test [34] for set-shifting abilities, among executive functions. Neuropsychology scores at baseline, contact zero and best contact are provided in Table S3.

Pre-surgical structural neuroimaging

Before surgery, structural and functional data were acquired for all patients on a 3T Siemens TRIO system (Siemens, Erlangen, Germany). A standard 8 channel head coil was used to acquire MPRAGE T1-weighted anatomical images with 1 mm^3 resolution [repetition time (TR), 2300 ms; echo time (TE), 2.98 ms; flip angle, 9°] and diffusion-weighted images (DWI). DWI acquisition was based on parameters used in previous probabilistic tractography studies of the basal ganglia [34]. Each volume consisted of 40 axial slices of 2.3 mm thickness with no interslice gaps and an acquisition matrix of 96 x 96 in a field of view (FoV) of 220 × 100 mm, resulting in 2.3 x 2.3 × 2.3 mm^3 isotropic voxels [TR, 5800 ms; TE, 103 ms; flip angle, 90°; bandwidth, 2004 Hz/pixel]. In order to increase signal-to-noise, we acquired two contiguous sequences of 128 diffusion-weighted images. Each dataset consisted of 64 images with diffusion gradients applied along 64 non-collinear encoding directions for two different diffusion sensitization strengths (b = 500, 100s/mm2), and one additional image with no

diffusion weighting (b = 0 s/mm2). A b value of zero delivers a T2-weighted EPI image for anatomical reference.

Pre-surgical functional neuroimaging

fMRI data acquisition

For each patient, 625 gradient-echo echo-planar T2*-weighted MR image volumes with blood oxygenation level-dependent (BOLD) contrast were acquired during symptom provocation, plus five additional volumes, acquired at the start of each session and subsequently discarded, to allow for T1 equilibration effects. Each whole-brain volume comprised 40 axial slices (2.2 mm thick; distance factor 0.25; TR 2.43 s; TE 30 ms; flip angle 90°) sequentially acquired (ascending).

Symptom-provocation fMRI experiment

In the context of fMRI scanning, all patients performed an OCD symptom provocation task. We employed a modified version of the OCD symptom-provocation paradigm using the Maudsley Obsessive–Compulsive Stimuli Set (MOCSS) developed by Mataix-Cols et al. [15,35]. During scanning, patients were presented with pictures of 4 classes of provocative stimuli, 50 of each type: 1) contamination/washing, 2) checking, 3) hoarding, 4) symmetry/order [15,35]. Examples of washing-related pictures included a public toilet, money, and a syringe. Examples of checking-related pictures included electric appliances (computer, kettle, light switch), an open door, and a purse. Examples of hoarding-related scenes included old newspapers/magazines, old clothes/toys, empty bottles/cans, and trash bins. Examples of symmetry-related scenes included books in a bookcase, a CD rack and a bathroom cabinet. In addition, 50 pictures of neutral scenes (e.g., furniture, nature scenes household items) were selected from a standard set of stimuli [36]. These stimuli had previously been carefully chosen [35] to avoid resembling common triggers of OCD symptoms. Note that 11 pictures of the MOCSS, pertaining to UK electrical plugs/sockets, money, cash-point and written English, were substituted for equivalent Spanish pictures obtained with a standard digital camera (Sony NEX-VG10E).

The study comprised 4 'blocks' pertaining to the 4 classes of provocative stimuli. Each block consisted of ten 20s alternating epochs in which subjects viewed either 10 provocative or 10 neutral pictures. Each picture was presented for 1950 ms (inter-stimulus interval 50 ms). Each epoch began with an 8 s period during which patients were played a prerecorded voice via MR-compatible headphones (VisuaStim XGA; Resonance Technology, Northridge, CA), instructing them to imagine being in a particular situation while looking at the scenes they were about to see (there were five slightly different recordings per type of stimuli in each experiment, to avoid monotony). We presented the same instructions as used previously [15], but recorded in Spanish. Some examples of these instructions are the following: For washing-related pictures: "Imagine that you must come into contact with what's shown in the following pictures without washing yourself afterward." For checking-related pictures: "Imagine that you are not sure whether you switched off or locked the following objects and it is impossible for you to go back and check." For hoarding-related pictures: "Imagine that the following objects belong to you and that you must throw them away forever." For symmetry-related pictures: "Imagine that you are not allowed to put the following items in order." For neutral scenes: "Imagine that you are completely relaxed while looking at the following scenes." After each set of pictures, another prerecorded sound file of the question "How anxious do you feel?" was played. Patients had to rate their subjective anxiety by pushing one of 5 buttons to indicate from 0 (no anxiety) to 4 (extreme anxiety).

Neurosurgical procedure

The day before the operation, a volumetric CT scan (Philips ® Brilliance 64 CT Scanner) was performed and fused with a contrast-enhanced T1 MRI and T2 volumetric images. The location of the posterior border of the anterior commissure (AC) and the anterior border of the posterior commissure (PC) were marked, and the target determined by measuring the distances from the AC-PC line and the mid-sagittal plane, using a Medtronic Stealth Station Treon navigation system (Medtronic Minneapolis, USA). The target for the NAcc was placed at the coordinates reported by Ref. [7]: 2.5 mm rostral to the anterior border of the anterior commissure, 4.5 mm ventral to the AC-PC line, and 6.5 mm lateral to the mid-sagittal plane. A trajectory was planned to reach the target point at the NAcc close to the bed nucleus of the stria terminalis (distal electrode or contact "0"), and for placing the rest of the contacts of a Medtronic Model 3391 stimulating macroelectrode at several points along the striatum avoiding the ventricles (contacts 1, 2, and 3; Fig. 1 and Figure S1).

On the operative day, a burr hole was performed on each side, the dura opened and the hole sealed with DuraSeal (DuraSeal Dural Sealant System, Confluent Surgical, Inc., Waltham, Massachusetts) to avoid CSF reflux. A microelectrode FC 4000 (FHC, Bowdoin, Maine, USA) was advanced into the ventral striatum towards the target using a Microdrive (Elekta MicroDrive™). In the case of relatively silent neuronal activity, the target was advanced 2 mm anteriorly. After microelectrode recording, the macroelectrode was implanted at the determined target, and the clinical effects were tested using an external tester (Medtronic Model 3625 Test Stimulator). Bipolar stimulation at 3.5 V between the most distal and the most proximal contacts (negative polarity most distal) was delivered at 130 Hz (pulse width 60 μs), and then increased up to 5 V to screen for undesired side effects (none of which appeared in any case). Intra-operative X-ray was used to verify the positioning of the two electrodes. Post-operative CT merged with preoperative MR verified final electrode position.

After implantation, the lead extensions were externalized and all possible combinations of the electrode leads were tested for their effectiveness using an external tester. After the external stimulation trial period, an Activa PC Model 37601 neurostimulator (Medtronic Inc) was implanted subcutaneously at the abdominal left flank and connected to the electrodes using an extension cable 33086 (Medtronic Inc).

Deep brain stimulation protocol

After surgery, a simple randomized sequence of contact activations (C0, 1, 2, 3) and sham (−), was generated for each patient. Each contact was stimulated at 130 Hz, pulse-width 60 μs, and 4.5 V for three months (the sham activation was 0 V) according to the patient's individual sequence, separated by one month of washout with the generator turned off (Fig. 1). The study meets a double-blind, longitudinal design. Stimulation contact was set following a random series known only by the neurosurgeon, whereas patient, psychiatry and neuropsychology teams were blinded. Some patients referred a transient sense of wellbeing when contact 0 was stimulated for the first time during stimulation trials prior to, but not during, the longitudinal study.

Statistical analysis

Statistical analysis of psychiatric and neuropsychological data

Psychiatric and neuropsychological scale results in the multiple stimulation periods were analyzed with repeated measures non-

parametric Friedman test. To evaluate pairwise significant differences between the pre-surgery scores, C0 score, and BC scores, non-parametric Wilcoxon's test was used. All statistical analyses were performed using IBM SPSS Statistics software version 20, and results considered significant at alpha level 0.05. Statistical parameters can be found in the Results section.

Neuroimaging analysis

fMRI data analysis

Functional imaging data were analyzed using statistical parametric mapping (SPM12; http://www.fil.ion.ucl.ac.uk/spm) employing an epoch-related model. Each imaging time series was realigned to correct for interscan movement, slice-time corrected, normalized into a standard anatomical space, and smoothed with a Gaussian kernel of 8 mm full width half-maximum. To test for symptom-provocation effects, we specified four effects of interest: the epochs corresponding to each symptom dimension. Epoch-specific responses were modeled by convolving a box-car function spanning epoch duration with a canonical hemodynamic response function (HRF) to create regressors of interest. Events corresponding to viewing instructions, and questions regarding anxiety levels, were modeled as separate regressors. Six movement parameters were modeled as nuisance covariates.

The predominant symptom(s) for each patient was defined (Table 1) and used to construct a contrast of responses to provocation relative to the neutral pictures baseline. The ensuing statistical parametric map for this contrast was thresholded at $P < 0.001$ uncorrected (unless otherwise stated). Note that due to weak responses during symptom activation in patients 4 and 6, the SPMs for these patients were first thresholded at $P < 0.01$ and 0.005 uncorrected, respectively. AlphaSim was used to correct for multiple comparisons at the cluster level ($P < 0.05$) for each patient. Alphasim thresholding was performed for the number of comparisons defined within a prefrontal mask accounting for the applied smoothing, (FWHM 8 mm). Different cluster thresholds (K) were obtained for the three pre-defined statistical thresholds: $P<0.01$ K>86; $P<0.005$ K>58; $P<0.001$ K>26. The prefrontal mask was created by combining the following regions from the Harvard-Oxford cortical atlas distributed with FSL (https://fsl.fmrib.ox.ac.uk/fsl/fslwiki): Superior Frontal Gyrus, Middle Frontal Gyrus, Inferior Frontal Gyrus pars triangularis and pars opercularis, Frontal Orbital Cortex, Supplementary motor cortex, Paracingulate Gyrus, Frontal Pole, Cingulate Gyrus (Anterior Division), Subcallosal Cortex, Frontal Operculum Cortex, and Frontal Medial Cortex.

Probabilistic tractography analysis

In a first step, each patient's electrode contacts were localized as follows. We extracted subject-specific volumetric masks of the caudate and accumbens nucleus in both hemispheres using an automated sub-cortical segmentation procedure in Freesurfer V5.1.0 [36]. Affine linear transformations between different image spaces were performed using FSL FLIRT [37]. Non-brain tissues were removed from T1-weighted images using FSL BET [38]. Post-operative CT images were thresholded to segment the skull and remove it from the unthresholded image and co-registered to the pre-operative T1-weighted image. The post-operative CT was again thresholded at an intensity of 1500 to retain just the electrodes in the T1-weighted image space. The contacts' coordinates were identified visually after superimposing the post-operative CT on the pre-operative T1-weighted MRI (Figure S1). A spherical region with a radius of 4 mm was then created at each contact coordinate.

Diffusion weighted imaging data were pre-processed using FSL BET [38] for non-brain tissue removal and FSL FDT for eddy currents correction [39]. Estimation of the diffusion parameters was performed using BEDPOSTX [40]. We used a multi-shell model for the fitting of the parameters [41]. White matter connectivity was quantified using probabilistic tractography with FDT Probtrackx 2.0 [42]. The contact spherical regions were used as seeds for the tractography analysis, and the fMRI activations were used as waypoints and termination masks. The rest of the parameters for the tractography analyses were kept as default, *i.e.,* 5000 streamlines per voxel, a maximum length of 2000 steps, minimum step length of 0.5 mm, and a curvature threshold of 80°. That is, we applied the default settings in FSL, standard in the field, in our tractography analyses.

For display of structural and functional overlap, tractographic terminations or fMRI activations were projected onto a cortical mesh using CARET (Computerized Anatomical Reconstruction Toolkit) software [43].

Pre-operative MRI index calculation

For a given electrode contact, or group of contacts, the MRI index, denoted as p(tracts), is the probability (%) of reaching the fMRI activation by seeding streamlines at the volume of activated tissues (VATs) of the electrode contact(s).

Table 1
Patient symptomatology and DBS effects within the study sample. "Main Obsessions" and "Main Compulsions" are defined as the most severe, resistant to treatment and disabling OCD symptoms at the time of recruitment for each patient (Pt). "Other OCD symptoms" are defined as concomitant OCD obsessions and compulsions with less degree of severity, resistance to treatment and disability. "Best contact" indicates the stimulation contact (0, 1, 2 or 3) along the electrode that yielded the lowest Y-BOCS score. "Y-BOCS pre", "Y-BOCS C0" and "Y-BOCS Best" pertain to the Y-BOCS score at baseline, following stimulation of contact 0, and following stimulation of the best contact, respectively. "% C0" and "% Best" pertain to the percentage of Y-BOCS score improvement with respect to baseline following stimulation of contact 0, and following stimulation of the best contact, respectively.

Pt	Main Obsessions	Main Compulsions	Other OCD Symptoms	Best contact	Y-BOCS pre	Y-BOCS C0	Y-BOCS Best	% C0	% Best
1	Doubts	Checking		2	36	19	1	47.22	97.22
2	Symmetry, Doubts	Ordering, Checking	Contamination/Cleaning	0,2	32	24	24	25.00	25.00
3	Contamination, Doubts	Cleaning Checking		2,3	29	17	16	41.38	44.83
4	Doubts, aggressive obsessive thoughts	Checking		2	24	23	11	4.17	54.17
5	Doubts	Checking	Contamination/Cleaning	3	38	32	20	15.79	47.37
6	Contamination	Cleaning	Symmetry/Ordering, Taboo thoughts, Hoarding	1	30	31	19	−3.33	36.67
7	Contamination	Cleaning	Doubts/Checking	2	37	29	17	21.62	54.05
Median Y-BOCS improvement across patients								21.62	47.37
Mean Y-BOCS improvement across patients								21.69	51.33
Percentage of responders (patients showing at least 35% reduction in Y-BOCS score)								28.57	85.71

Results

The most effective striatal stimulation site varies between patients

Electrodes were successfully placed along a striatal axis in all patients, with two contacts in NAcc (C0, C1) and two in the caudate head (C2, C3), bilaterally. This is evident on inspecting the fusion of each patient's post-operative computed tomography (CT) scan with the pre-operative structural MRI (Figure S1). Across the 7 patients, the main obsession(s) and compulsion(s) showed heterogeneity (Table 1). For each patient, the contact yielding lowest Y-BOCS score achieved during the longitudinal study was labeled as "best" contact (BC). The neuroanatomical locus of the BC varied between patients (Table 1, Table S2) and was more frequently observed in caudate than accumbens nucleus (Table S3, Figure S2). According to current convention [45], patients with a Y-BOCS score decrease of more than 35% with respect to baseline are considered DBS responders. Of the seven patients studied, clinical improvement following BC stimulation exceeded 35% in six patients (Table 1), with a median (Mdn) Y-BOCS reduction of 47.37% at their BC. Directly contrasting this finding against clinical efficacy of the commonly stimulated most distal contact (C0) in the NAcc, we observe that across the group, stimulation of C0 achieved a Mdn Y-BOCS reduction of 21.62% (Table S3). Only two participants (28.57%) would have been classified as responders if C0 alone had been stimulated, and in both cases (Patients 1 and 3), the BC was not in contact 0 (Table 1), *i.e.,* stimulation at more dorsal striatal sites were more effective in these patients.

Differential clinical response as a function of stimulated contact was confirmed by a Friedman Test on Y-BOCS scores for all stimulation trials, baseline and sham across the 7 patients ($\chi2(5) = 17.941$, $P = 0.003$, Kendall W = 0.513). Post-hoc Wilcoxon signed-rank tests were first performed to test for improvement relative to pre-surgical baseline for all stimulated contacts and sham. Across the 7 patients, compared to pre-surgical evaluation (Mdn- $\text{Baseline}_{\text{Y-BOCS}} = 32$), stimulation at C0 (Mdn-$\text{C0}_{\text{Y-BOCS}} = 24$), C1 (Mdn-$\text{C1}_{\text{Y-BOCS}} = 22$), C2 (Mdn-$\text{C2}_{\text{Y-BOCS}} = 17$), C3 (Mdn-$\text{C3}_{\text{Y-BOCS}} = 22$) and sham (Mdn-$\text{Sham}_{\text{Y-BOCS}} = 20$) stimulation all produced a significant decrease in Y-BOCS scores ($Z = -2.120$, $P = 0.034$, effect size r = 0.801; $Z = -2.371$, $P = 0.018$, r = 0.896; $Z = -2.371$, $P = 0.018$, r = 0.896; $Z = -2.375$, $P = 0.018$, r = 0.897; $Z = -2.366$, $P = 0.018$, r = 0.894 for C0, C1, C2, C3 and Sham *vs.* Baseline, respectively). Next, post-hoc Wilcoxon tests were performed on percent improvement in Y-BOCS score at BC, contact Zero and Sham (each relative to baseline). Specifically confirming our hypothesis that BC outperforms NAcc C0 stimulation, the percentage Y-BOCS score improvement was significantly greater at BC (Mdn-$\text{BC}_{\text{Y-BOCS}}$ decrease = 47.37%) than at C0 (Mdn-$\text{C0}_{\text{Y-BOCS}}$ decrease = 21.62%) ($Z = -2.207$, $P = 0.027$, r = 0.834). There was a trend in Y-BOCS improvement at BC relative to sham stimulation (Mdn-ShamY-BOCS = 25.00%) ($Z = -1.859$, $P = 0.063$, r = 0.702), stimulation at C0 yielded actually marginally less Y-BOCS improvement than during Sham ($Z = -1.782$, $P = 0.075$, r = 0.673). We note, however, that Patient 3 underwent a major life event during her Sham period (discussed below). Repeating the Wilcoxon test excluding this patient shows a significant improvement of BC over Sham stimulation ($Z = -1.992$, $P = 0.046$, r = 0.752) and no Y-BOCS improvement difference between C0 and Sham stimulation ($Z = -1.483$, $P = 0.138$).

We note that in Patients 3 and 7, it is quite probable that the most distal electrode contact is placed at the ventricles (Figure S1). In neither case was this contact (C0) the most effective contact. Y-BOCS reduction following stimulation this distal contact was either at the same level (Patient 7) or less than (Patient 3) that observed during sham stimulation.

In addition to our primary outcome measure (Y-BOCS), anxiety measures were collected using the STAI state scale and Hamilton anxiety rating scale (HAM-A) at all evaluation periods in Patients 4 to 7. A Friedman Test on these scores for all stimulation trials, baseline and sham across the 4 patients showed a significant effect for HAM-A ($\chi2(5) = 11.143$, $P = 0.049$). Additionally, there was a trend in STAI-state improvement ($\chi2(5) = 10.857$, $P = 0.054$) under the best contact relative to the rest of the trials. For both scores, post-hoc Wilcoxon tests comparing each stimulation period with baseline, or BC with baseline, did not reveal any significant effects.

Striatal stimulation has limited effects on cognitive function

DBS at different striatal sites produced limited effects on cognitive testing. For each neuropsychological test (Table S4), scores as a function of stimulated contact were entered into a Friedman Test for all stimulation trials, baseline and sham across the 7 patients. Statistically significant effects were only observed for Trail Making Test-B (TMT-B) performance times ($\chi2(5) = 13.787$, $P = 0.017$, Kendall W = 0.460). Post-hoc Wilcoxon signed-rank tests were performed on scores relative to pre-surgical baseline for all stimulated contacts and sham. Across the 7 patients, compared to pre-surgical evaluation (Mdn-$\text{Baseline}_{\text{TMT-B-Time}} = 155$ s) stimulation at C0 (Mdn-$\text{C0}_{\text{TMT-B-Time}} = 77$ s), C1 (Mdn-$\text{C1}_{\text{TMT-B-Time}} = 62.5$ s), and sham (Mdn-$\text{Sham}_{\text{TMT-B-Time}} = 66$ s) stimulation produced a significant decrease in TMT-B performance time ($Z = -2.366$, $P = 0.018$, r = 0.894; $Z = -1.992$, $P = 0.046$, r = 0.752; $Z = -2.366$, $P = 0.018$, r = 0.894, for C0, C1 and Sham *vs.* Baseline, respectively). Next, post-hoc Wilcoxon tests were performed on performance times at BC, C0 and Sham, relative to baseline. However, TMT-B performance time following BC (Mdn-$\text{BC}_{\text{TMT-B-Time}} = 88$ s) was not significantly different from baseline ($P = 0.866$). A Kruskal-Wallis H Test was run to test for a learning effect in TMT-A and TMT-B performance time across the 6 repetitions of the test performed during the study period. Results indicated no significant repetition effect in TMT-A ($\chi2(5) = 2.691$, $P = 0.748$) or in TMT-B scores ($\chi2(5) = 6.345$, $P = 0.274$).

Pre-operative MRI index predicts optimal stimulation site

The analysis of haemodynamic responses during symptom provocation measured with fMRI was limited to the most symptomatic dimension(s) for each patient. Relative to a control condition (presentation of neutral pictures), viewing predominant symptom-related images produced frontal activation in all patients, of varying magnitude and neuroanatomical locus (Fig. 2). Note that different prefrontal regions are activated, even when comparing patients with the same predominant symptom. For each patient, probabilistic tractography was performed by placing seed regions around each of the 4 electrode contacts and using patient-specific frontal activations as target regions (Fig. 3). The volume of activated tissue (VAT) for monopolar stimulation of each contact was approximated as a sphere of diameter 4 mm around the contact [46]. That is, connectivity between each of the contacts and that patient's fMRI activations was calculated as the probability of fibers projecting from each contact VAT to the cortical activated areas [44].

The analysis proceeded in a hierarchical manner, first examining whether our pre-operative MRI index could dissociate whether the BC was in NAcc or caudate, and secondly testing whether this index could determine BC identity between the two contacts within-region. Thus, in a first step, we calculated for each patient, the probability of fibers projecting to the activated prefrontal areas, where this projection arises from a combination of VATs from NAcc contacts (C0 and C1) or caudate contacts (C2 and C3). Y-BOCS

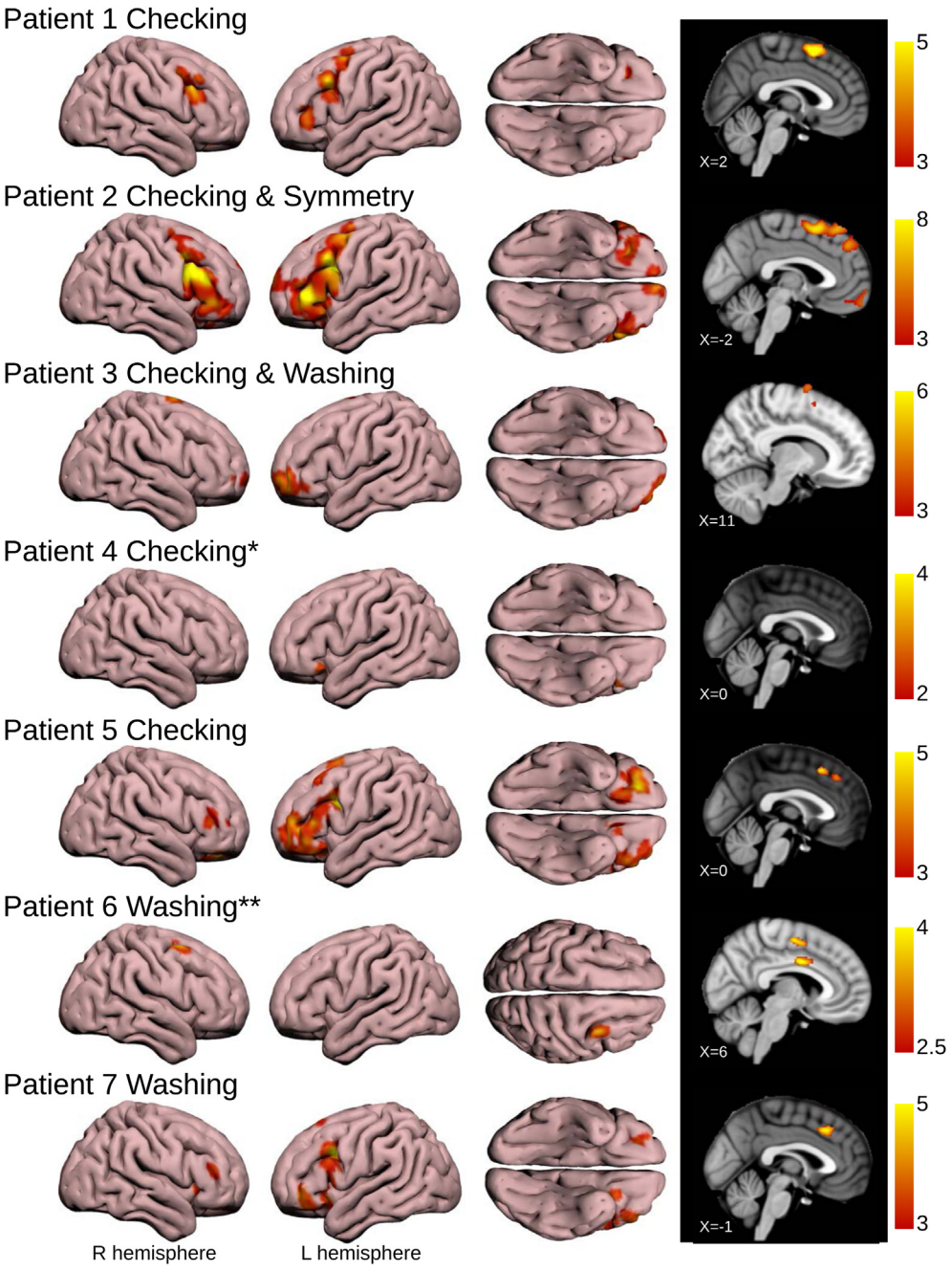

Fig. 2. Individual patient BOLD responses during symptom provocation. For each patient, the response to their most prominent symptom dimension (relative to baseline) is shown (masked to include only the prefrontal cortex). For patients with multiple prominent symptoms, provoked responses to each have been averaged. Statistical parametric maps are overlaid on a canonical rendering (left 3 panels) and on a midline sagittal section (right panel). All statistical parametric maps are displayed at uncorrected height threshold $P < 0.001$, unless indicated ($^{*}P < 0.01$, $^{**}P < 0.005$), with cluster extent determined by AlphaSim correction at $P < 0.05$. Colorbars indicate the *T*-statistic of the activation. L: left, R: right.

reduction was also averaged for the 2 contacts in each region. The clinically most effective striatal area coincided in six out of seven cases with the probabilistic tractography projections from the activated prefrontal areas (Table 2). The only patient in whom the MRI index did not coincide with maximal Y-BOCS reduction is Patient 2, who is the only patient not classified as a responder to DBS at any contact. Thus, limiting our sample to responder patients, all 6 from 6 patients' pre-operative MRI indices coincide with maximal Y-BOCS reduction (Binomial test, $P = 0.031$). By contrast, the pre-operative MRI index only predicted which of the two contacts within-region was most efficacious in 4 of 6 patients, which was not significantly above chance levels (Binomial test, $P = 0.688$).

An alternative account of our findings would be that, due to individual differences in anatomical connectivity and electrode localization, the notion of best contact arises simply because a key area of PFC is structurally connected with the BC VAT, which overlaps across patients. If this were the case, we would expect that tractographic projections from the VAT of each BC would show overlap in all 6 responders. This was not the case (Fig. 4A), with maximum overlap expressed in right ventral frontal pole but

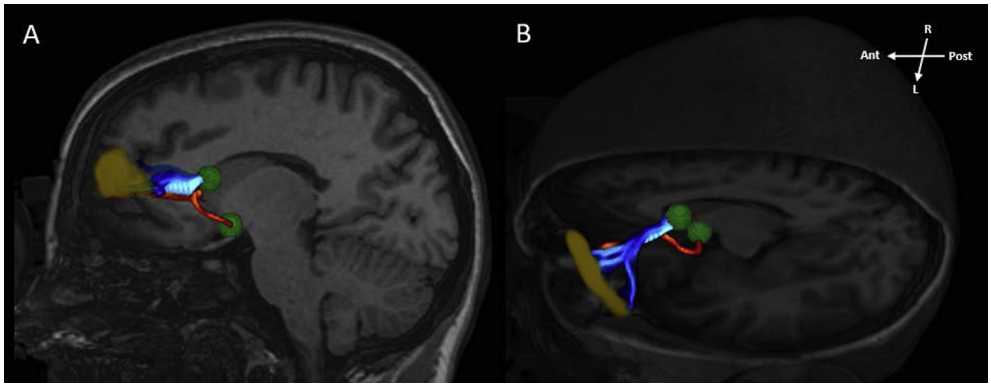

Fig. 3. Probabilistic tractography from electrode contact to frontal activation. The tracts projecting from the volume of activated tissue for 2 left-sided electrode contacts (green spheres) to the left prefrontal area activated to prevailing symptom provocation (brown) are illustrated for one example case (Patient 3) in sagittal (**A**) and 3-dimentional overhead oblique transverse (**B**) section. The number of streamlines from the dorsal contact C3 (light blue) that reach the activated prefrontal area is greater than the equivalent projection (red) from the ventral C0 contact in the nucleus accumbens. In this patient, C3 was, together with C2, the most efficacious (or "best") contact. Ant: anterior, Post: posterior, L: left, R: right. (For interpretation of the references to color in this figure legend, the reader is referred to the Web version of this article.)

Table 2
Pre-operative structural-functional MRI index determines in which neuroanatomical locus DBS will lead to most reduction in Y-BOCS. Pt: Patient. p(tracts): probability (%) of reaching the fMRI activation by seeding streamlines at the volume of activated tissues (VATs) of each specific electrode contact. % Y-BOCS ↓: percent reduction in Y-BOCS score following stimulation of a structure (Nacc or Caudate, expressed as average Y-BOCS reduction following stimulation of C0 and C1 or C2 and C3, respectively) or following stimulation of individual contacts within a structure (ventral or dorsal contacts).

Pt	NAcc (contacts C0,C1)		Caudate (contacts C2,C3)		Contact	Does best %Y-BOCS ↓ coincide with higher p(tracts)?	Ventral contact		Dorsal contact		Does best %Y-BOCS ↓ coincide with higher p(tracts)?
	p(tracts)	% Y-BOCS ↓	p(tracts)	% Y-BOCS ↓	BC		p(tracts)	% Y-BOCS ↓	p(tracts)	% Y-BOCS ↓	
1	0.014	43.06	4.761	68.06	2	Yes - in Caudate	C2 0.008	C2 97.22	C3 9.514	C3 38.89	Yes – C3
2	3.200	17.19	16.762	15.63	0, 2	No					
3	1.973	36.21	4.812	44.83	2, 3	Yes - in Caudate	C2 4.795	C2 44.83	C3 4.830	C3 44.83	Yes – C2/C3
4	0.016	16.67	0.039	29.17	2	Yes - in Caudate	C2 0.012	C2 54.17	C3 0.067	C3 4.17	No
5	6.619	30.26	3.661	25.00	3	Yes - in NAcc	C0 1.912	C0 15.79	C1 11.327	C1 44.74	Yes – C1
6	0.117	16.67	0.067	8.33	1	Yes - in NAcc	C0 0.198	C0 −3.33	C1 0.037	C1 36.67	No
7	0.008	28.38	0.058	51.35	2	Yes - in Caudate	C2 0.027	C2 54.05	C3 0.088	C3 48.65	Yes – C3

limited to 5 of 6 patients. Note that this analysis took C2 as BC for Patient 3; if C3 is taken as BC (both contacts produced equal Y-BOCS improvement in this patient) the maximum overlap in prefrontal projections again observed in this ventral frontal polar region but only in 4 of the 6 patients. This argues against an explanation of our findings in terms of BC connectivity to a specific frontal area. Furthermore, there was even less overlap across patients for predominant symptom-evoked fMRI responses, with a maximum of 4 out of 6 patient overlap in several prefrontal areas (Fig. 4B), with no overlap in right ventral frontal pole.

Discussion

Current debate is focused on which of the DBS targets for OCD – ALIC, VC/VS, NAcc, limbic STN, or ITP – is the single most efficacious target for all possible cases of OCD [7–11]. However, the response rates to DBS to all of these targets in OCD is relatively low (50%) and equivalent to that following stereotactic lesions of different targets along the limbic circuit and its prefrontal projections [18,45]. By adopting an alternative strategy, focusing on the symptom content of each patient, we demonstrate that the optimal stimulating electrode contact location for DBS in each OCD patient is not at a fixed anatomical locus within the ventral striatum or NAcc, but rather at different points along the striatum. This optimal stimulation site varies between patients. Symptom provocation activates specific sites of the prefrontal cortex. For example, patients with contamination obsessions mainly activate the medial orbitofrontal (ventromedial) cortex, while those who present checking symptoms chiefly activate the dorsolateral prefrontal cortex (PFC) [15]. Tracing probabilistic tractography projections from a seed defined as the volume of activated tissue of each contact towards the prefrontal cortex yields a probability to hit the activated sites' volumes for each contact (referred to here as the MRI index). In 6 of 7 cases, the most effective structure (accumbens or caudate) was the one with the highest MRI index. Thus, stimulating at this optimal contact location instead of at a fixed target increases the chance of clinical response to DBS from the typical response rate of 50% [21,22], to a rate of ~86% described here. It is relevant to stress that response rates in literature are quite varied. Kohl's study stated that the average rate of responders in NAc stimulation was 45.5% [21], whereas Alonso's revision [22] mentioned some successful single case studies (Kuhn et al., 2007, Grant et al., 2012 and Sachdev et al., 2012), more successful trials as the Denys et al., 2010 (9 out of 16) and low success studies such as Huff et al., 2010 (1 responder out of 10).

The observation that patients with different symptom content respond to specific stimulation locations along a dorsoventral striatal axis raises a possibility that this concept is applicable to other DBS targets. For example, the ALIC is topographically organized following the same pattern as the fronto-striatal projections

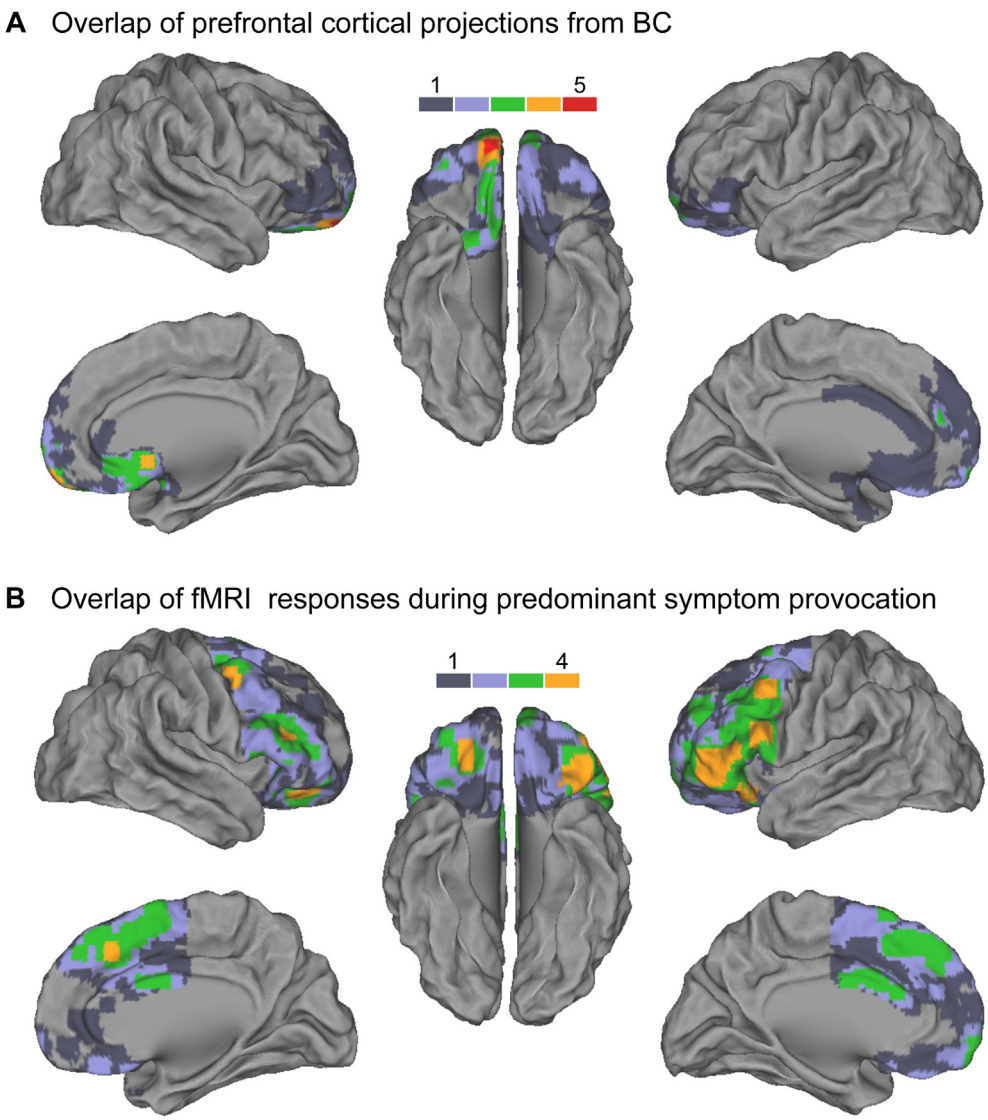

Fig. 4. Structural and functional overlap across responders (*n*=6). (**A**) For each patient showing a clinical response to DBS, the prefrontal termination of tracts seeded from their best contact was thresholded at $P < 0.001$ and projected onto a cortical mesh. The overlap of these terminations, over patients, is indicated by the color code. Note that only a small region in the right frontal pole reaches an overlap of 5 patients. (**B**) For each patient, the prefrontal response to their most prominent symptom dimension (relative to baseline) was thresholded at $P < 0.05$ uncorrected and projected onto a cortical mesh. Again, frequency maps were created by combining the thresholded maps of the six subjects. Here, the maximum overlap was only 4 patients. (For interpretation of the references to color in this figure legend, the reader is referred to the Web version of this article.)

[46]. Effectiveness in other targets may, however, vary due to the fact that in these structures the different subregions (*e.g.*, limbic *vs.* associative STN) are more densely packed, so it is possible that several topographically distinct subregions, and their associated connections, are within the same contact's volume of activated tissue. Stimulation of structures that do not contribute to the patient's individual pathology could be related to the appearance of reduced therapeutic effect or to side effects. For example, in OCD patients treated with ALIC-DBS, stimulation of specific fiber tracts is associated with Y-BOCS improvement, but the overall amount of fiber activation may be inversely correlated with therapeutic effect [44].

We did not record any neuropsychological adverse effects after stimulation of the striatum, nor recorded seizures. Although some reports warn against cognitive effects from traversing or stimulating the caudate [47], others have demonstrated that the striatum can be traversed without major cognitive complications [48], as was the case for our patient group. Overall, the stimulation of more dorsal striatal contacts proved more efficacious in our sample than the more ventral or accumbens ones. This could reflect a particular skew towards more “associative” symptoms (checking, symmetry) present in our patient sample than “limbic” ones (washing) Although most authors claim that the most effective contacts are C0 and C1 in all patients, in some studies up to 30% of patients responded best to stimulation in contacts C2 and C3 [49–51].

We met several methodological problems during this study. Firstly, the number of cases is small, and the design is very demanding for the patients, since they had to go through five different study periods, which were necessarily short (3 months) to avoid the overall study being too long (already 19 months with study periods of 3 months). During short study periods, personal events and other factors unrelated to the stimulation could have strongly biased the results (in our sample, one patient had a termination of pregnancy, another patient suffered the death of a

brother, and a third patient started a new romantic relationship during the study span). Secondly, although the study was randomized and double-blind, we cannot discard a placebo effect contributing to our results. Note that the Y-BOCS scores during the zero volt (sham) period did not return to pre-surgical baseline values. The fact that the mean improvement in contacts apart from the BC is similar to sham stimulation leads us to think that BC stimulation effectively evokes clinical improvement, whereas improvement during the other stimulations is due to a placebo effect or to a carry-over therapeutic benefit from the previous stimulation period. Thirdly, as the Y-BOCS does not distinguish in its overall score between the different symptomatic dimensions, these dimensions have not been measured by the primary outcome variable. Subsequently, if for example contamination/cleaning symptoms improve but doubt/checking do not, the improvement in the former may not be reflected in the overall Y-BOCS score. Fourthly, stimulation was bilateral, despite symptom provocation fMRI often showing an asymmetric distribution of prefrontal activation. Unilateral stimulation trials would have further increased the duration of the study. Fifth, we used voltage setting for our electrodes, but intensity settings might have been better in avoiding the effect of changes in conductivity. However, we did not observe important differences in impedances tested among the contacts within each patient, among the different patients, or along the different periods of the study. Lastly, the MOCSS-fMRI paradigm is validated for groups of patients whereas we used this test for individual patients, with 2 patients showing relatively weak activation patterns in the frontal lobe.

By considering the "best" contact, 6 out of 7 patients with severe OCD were classified as responders to DBS. The location of the best contact varied over patients, but – critically – the most effective neuroanatomical target structure coincided with a pre-operative MRI index derived from OCD functional MRI symptom provocation combined with probabilistic tractography. We therefore show that the optimal target OCD DBS is not the same for all cases, but varies in an individualized, content-specific and predictable manner. These results support models of cortico-striatal loops underlying the pathophysiology of OCD. Moreover, they demonstrate the efficacy of an innovative therapeutic strategy, recommending a change in target-selection for functional neurosurgery in psychiatric patients away from established fixed targets for all cases in one disease – which only yields an average 50% response to DBS in resistant OCD – to a more personalized approach based on physiological and anatomical data. Since the sample studied is relatively small, this method should be confirmed further with a higher number of patients, measuring DBS-evoked longitudinal changes of the individual dimensions of each patient. In general, employing a combination of functional imaging and tractography may represent a step towards personalized functional neurosurgery.

Author contributions

Conceptualization, JAB; Methodology, JAB, JMA-C, JAPP, BR and BAS; Investigation, JAB, JMA-C, CN, RA, JG-A, BR, BAS; Writing – Original Draft, JAB, CN and BAS; Writing – Review & Editing, JMA-C, RA, JG-A, JAPP and BR; Funding Acquisition, JAB and BAS; Supervision, JAB, BR and BAS.

Conflict of interest policies

JAB reports having received research funding from Boston Scientific and Medtronic. CN is funded by Boston Scientific. All other authors reported no biomedical financial interests or potential conflicts of interest.

Acknowledgements

This work was supported by the FIS PI10/01932 project, integrated in the AcciEstraégica den Salud AES 2010, funded by the ISCIII and co-funded by the European Regional Development Fund (ERDF) to JAB. BAS is supported by the Spanish Ministry of Economy and Competitiveness (MINECO) (Project grant SAF2015-65982-R). We would like to thank the Methodology Unit of Hospital Clínico San Carlos for their support.

Appendix A. Supplementary data

Supplementary data to this article can be found online at https://doi.org/10.1016/j.brs.2018.12.226.

References

[1] Blomstedt P, Sjöberg RL, Hansson M, Bodlund O, Hariz MI. Deep brain stimulation in the treatment of obsessive-compulsive disorder. World Neurosurg 2013;80. https://doi.org/10.1016/j.wneu.2012.10.006.
[2] Denys D. Deep brain stimulation of the nucleus accumbens for treatment-refractory. Obsessive-Compulsive Disord 2014;67:1061–8.
[3] Pepper J, Hariz M, Zrinzo L. Deep brain stimulation versus anterior capsulotomy for obsessive-compulsive disorder: a review of the literature. J Neurosurg 2015;122:1028–37. https://doi.org/10.3171/2014.11.JNS132618.
[4] van Westen M, Rietveld E, Figee M, Denys D. Clinical outcome and mechanisms of deep brain stimulation for obsessive-compulsive disorder. Curr Behav Neurosci Rep 2015;2:41–8. https://doi.org/10.1007/s40473-015-0036-3.
[5] Murray CJL, Lopez AD. The global burden of disease: a comprehensive assessment of mortality and disability from diseases, injuries, and risk factors in 1990 and projected to 2020. Glob. Burd. Dis. Inj. Ser. Harvard Sc. Cambridge, MA: Harvard Univ. Press; 1996.
[6] Kessler RC, Berglund P, Demler O, Jin R, Merikangas KR, Walters EE. Lifetime prevalence and age-of-onset distributions of DSM-IV disorders in the national comorbidity survey replication. Arch Gen Psychiatr 2005;62:593–602. https://doi.org/10.1001/archpsyc.62.6.593.
[7] Sturm V, Lenartz D, Koulousakis A, Treuer H, Herholz K, Klein JC, et al. The nucleus accumbens: a target for deep brain stimulation in obsessive-compulsive- and anxiety-disorders. J Chem Neuroanat 2003;26:293–9. https://doi.org/10.1016/j.jchemneu.2003.09.003.
[8] Greenberg BD, Gabriels L a, Malone D a, Rezai a R, Friehs GM, Okun MS, et al. Deep brain stimulation of the ventral internal capsule/ventral striatum for obsessive-compulsive disorder: worldwide experience. Mol Psychiatr 2010;15:64–79. https://doi.org/10.1038/mp.2008.55.
[9] Mallet L, Polosan M, Jaafari N, Baup N, Welter M-L, Fontaine D, et al. Subthalamic nucleus stimulation in severe obsessive-compulsive disorder. N Engl J Med 2008;359:2121–34. https://doi.org/10.1056/NEJMoa0708514.
[10] Nuttin B, Cosyns P, Demeulemeester H, Gybels J, Meyerson B. Electrical stimulation in anterior limbs of internal capsules in patients with obsessive-compulsive disorder. Lancet 1999;354:1526. https://doi.org/10.1016/S0140-6736(99)02376-4.
[11] Jimenez-Ponce F, Velasco-Campos F, Castro-Farfan G, Nicolini H, Velasco AL, Salin-Pascual R, et al. Preliminary study in patients with obsessive-compulsive disorder treated with electrical stimulation in the inferior thalamic peduncle. Neurosurgery 2009;65:203–9. https://doi.org/10.1227/01.NEU.0000345938.39199.90. discussion 209.
[12] Lipsman N, Neimat JS, Lozano AM. Deep brain stimulation for treatment-refractory obsessive-compulsive disorder: the search for a valid target. Neurosurgery 2007;61:1–11. https://doi.org/10.1227/01.neu.0000279719.75403.f7.
[13] Bloch MH, Landeros-Weisenberger A, Rosario MC, Pittenger C, Leckman JF. Meta-analysis of the symptom structure of obsessive-compulsive disorder. Am J Psychiatry 2008;165:1532–42. https://doi.org/10.1176/appi.ajp.2008.08020320.
[14] Matsunaga H, Hayashida K, Kiriike N, Maebayashi K. The clinical utility of symptom dimensions in obsessive-compulsive disorder. Psychiatr Res 2010;180:25–9. https://doi.org/10.1016/j.psychres.2009.09.005.
[15] Mataix-Cols D, Wooderson S, Lawrence N, Brammer MJ, Speckens A, Phillips ML. Distinct neural correlates of washing, checking, and hoarding symptom dimensions in obsessive-compulsive disorder. Arch Gen Psychiatr 2004;61:564–76. https://doi.org/10.1001/archpsyc.61.6.564.
[16] Lehman JF, Greenberg BD, McIntyre CC, Rasmussen SA, Haber SN. Rules ventral prefrontal cortical axons use to reach their targets: implications for diffusion tensor imaging tractography and deep brain stimulation for psychiatric illness. J Neurosci 2011;31:10392–402. https://doi.org/10.1523/JNEUROSCI.0595-11.2011.
[17] Haber SN, Knutson B. The reward circuit: linking primate anatomy and human imaging. Neuropsychopharmacology 2009;35:4–26. https://doi.org/10.1038/npp.2009.129.

[18] Mcgovern R, Sameer S. Role of the dorsal anterior cingulate cortex in obsessive-compulsive disorder: converging evidence from cognitive neuroscience and psychiatric neurosurgery. Rev J Neurosurg 2017;126:132. https://doi.org/10.3171/2016.1.JNS15601.
[19] Rotge J-Y, Guehl D, Dilharreguy B, Cuny E, Tignol J, Bioulac B, et al. Provocation of obsessive-compulsive symptoms: a quantitative voxel-based meta-analysis of functional neuroimaging studies. J Psychiatry Neurosci 2008;33:405–12.
[20] Menzies L, Chamberlain SR, Laird AR, Thelen SM, Sahakian BJ, Bullmore ET. Integrating evidence from neuroimaging and neuropsychological studies of obsessive-compulsive disorder: the orbitofronto-striatal model revisited. Neurosci Biobehav Rev 2008;32:525–49. https://doi.org/10.1016/j.neubiorev.2007.09.005.
[21] Kohl S, Schönherr DM, Luigjes J, Denys D, Mueller UJ, Lenartz D, et al. Deep brain stimulation for treatment-refractory obsessive compulsive disorder: a systematic review. BMC Psychiatry 2014;14:1–10. https://doi.org/10.1186/s12888-014-0214-y.
[22] Alonso P, Cuadras D, Gabrils L, Denys D, Goodman W, Greenberg BD, et al. Deep brain stimulation for obsessive-compulsive disorder: a meta-analysis of treatment outcome and predictors of response. PLoS One 2015;10:1–16. https://doi.org/10.1371/journal.pone.0133591.
[23] Limousin P, Speelman JD, Gielen F, Janssens M. Multicentre European study of thalamic stimulation in parkinsonian and essential tremor. J Neurol Neurosurg Psychiatry 1999;66:289–96. https://doi.org/10.1136/jnnp.66.3.289.
[24] Goodman WK, Price LH. Assessment of severity and change in obsessive compulsive disorder. Psychiatr Clin North Am 1992;15:861–9.
[25] Pedersen G, Karterud S. The symptom and function dimensions of the Global Assessment of Functioning (GAF) scale. Compr Psychiatr 2012;53:292–8. https://doi.org/10.1016/j.comppsych.2011.04.007.
[26] Guy W. ECDEU Assess Man Psychopharmacol Vol DHEW Publ No ADM 76. Clinical Global Impression Scale, 338; 1976. p. 218–22.
[27] Grober E, Buschke H, Crystal H, Bang S, Dresner R. Screening for dementia by memory testing. Neurology 1988;38:900–3. https://doi.org/10.1212/WNL.38.6.900.
[28] MacLeod CM. Half a century of research on the Stroop effect: an integrative review. Psychol Bull 1991;109:163–203. https://doi.org/10.1037//0033-2909.109.2.163.
[29] Benton AL. Differential behavioral effects in frontal lobe disease. Neuropsychologia 1968;6:53–60. https://doi.org/10.1016/0028-3932(68)90038-9.
[30] Goodglass H, Kaplan E. Assessment of aphasia and related disorders. Philadelphia: Lea & Febiger; 1972.
[31] Isaacs B, Kennie AT. The set test as an aid to the detection of dementia in old people. Br J Psychiatry 1973;122:467–70. https://doi.org/10.1192/bjp.123.4.467.
[32] Wecchler D, Coalson DL, Raiford ES. WAIS–IV: Wechsler adult intelligence scale. San Antonio, TX: Pearson; 2008.
[33] Rabin LA, Barr WB, Burton LA. Assessment practices of clinical neuropsychologists in the United States and Canada: a survey of INS, NAN, and APA Division 40 members. Arch Clin Neuropsychol 2005;20:33–65. https://doi.org/10.1016/j.acn.2004.02.005.
[34] Berg EA. A simple objective technique for measuring flexibility in thinking. J Gen Psychol 1948;39:15–22. https://doi.org/10.1080/00221309.1948.9918159.
[35] Mataix-Cols D, Cullen S, Lange K, Zelaya F, Andrew C, Amaro E, et al. Neural correlates of anxiety associated with obsessive-compulsive symptom dimensions in normal volunteers. Biol Psychiatry 2003;53:482–93. https://doi.org/10.1016/S0006-3223(02)01504-4.
[36] Fischl B, Salat DH, Busa E, Albert M, Dieterich M, Haselgrove C, et al. Whole brain segmentation: automated labeling of neuroanatomical structures in the human brain. Neuron 2002;33:341–55. https://doi.org/10.1016/S0896-6273(02)00569-X.
[37] Jenkinson M, Smith S. A global optimisation method for robust affine registration of brain images. Med Image Anal 2001;5:143–56. https://doi.org/10.1016/S1361-8415(01)00036-6.
[38] Smith SM. Fast robust automated brain extraction. Hum Brain Mapp 2002;17:143–55. https://doi.org/10.1002/hbm.10062.
[39] Lai CH, Wu Y Te, Yu PL, Yuan W. Improvements in white matter microstructural integrity of right uncinate fasciculus and left fronto-occipital fasciculus of remitted first-episode medication-naïve panic disorder patients. J Affect Disord 2013;150:330–6. https://doi.org/10.1016/j.jad.2013.04.014.
[40] Behrens TEJ, Woolrich MW, Jenkinson M, Johansen-Berg H, Nunes RG, Clare S, et al. Characterization and propagation of uncertainty in diffusion-weighted MR imaging. Magn Reson Med 2003;50:1077–88. https://doi.org/10.1002/mrm.10609.
[41] Jbabdi S, Sotiropoulos SN, Savio AM, Graña M, Behrens TEJ. Model-based analysis of multishell diffusion MR data for tractography: how to get over fitting problems. Magn Reson Med 2012;68:1846–55. https://doi.org/10.1002/mrm.24204.
[42] Behrens TEJ, Berg HJ, Jbabdi S, Rushworth MFS, Woolrich MW. Probabilistic diffusion tractography with multiple fibre orientations: what can we gain? Neuroimage 2007;34:144–55. https://doi.org/10.1016/j.neuroimage.2006.09.018.
[43] Van Essen DC, Drury HA, Dickson J, Harwell J, Hanlon D, Anderson CH. An integrated software suite for surface-based analyses of cerebral cortex. J Am Med Inf Assoc 2001;8:443–59. https://doi.org/10.1136/jamia.2001.0080443.
[44] Hartmann CJ, Lujan JL, Chaturvedi A, Goodman WK, Okun MS, McIntyre CC, et al. Tractography activation patterns in dorsolateral prefrontal cortex suggest better clinical responses in OCD DBS. Front Neurosci 2016;9. https://doi.org/10.3389/fnins.2015.00519.
[45] Tomlinson CL, Stowe R, Patel S, Rick C, Gray R, Clarke CE. Systematic review of levodopa dose equivalency reporting in Parkinson's disease. Mov Disord 2010;25:2649–53. https://doi.org/10.1002/mds.23429.
[46] Safadi Z, Grisot G, Jbabdi S, Behrens T, Heilbronner SR, McLaughlin NCR, et al. Functional segmentation of the anterior limb of the internal capsule: linking white matter abnormalities to specific connections. J Neurosci 2018. https://doi.org/10.1523/JNEUROSCI.2335-17.2017.
[47] Witt K, Granert O, Daniels C, Volkmann J, Falk D, Van Eimeren T, et al. Relation of lead trajectory and electrode position to neuropsychological outcomes of subthalamic neurostimulation in Parkinson's disease: results from a randomized trial. Brain 2013;136:2109–19. https://doi.org/10.1093/brain/awt151.
[48] Mulders AEP, Plantinga BR, Schruers K, Duits A, Janssen MLF, Ackermans L, et al. Deep brain stimulation of the subthalamic nucleus in obsessive-compulsive disorder: neuroanatomical and pathophysiological considerations. Eur Neuropsychopharmacol 2016;26:1909–19. https://doi.org/10.1016/j.euroneuro.2016.10.011.
[49] Aouizerate B, Cuny E, Bardinet E, Yelnik J, Martin-Guehl C, Rotge J-Y, et al. Distinct striatal targets in treating obsessive-compulsive disorder and major depression. J Neurosurg 2009;111:775–9. https://doi.org/10.3171/2009.2.JNS0881.
[50] Goodman WK, Foote KD, Greenberg BD, Ricciuti N, Bauer R, Ward H, et al. Deep brain stimulation for intractable obsessive compulsive disorder: pilot study using a blinded, staggered-onset design. Biol Psychiatry 2010;67:535–42. https://doi.org/10.1016/j.biopsych.2009.11.028.
[51] Greenberg BD, Malone DA, Friehs GM, Rezai AR, Kubu CS, Malloy PF, et al. Three-year outcomes in deep brain stimulation for highly resistant obsessive-compulsive disorder. Neuropsychopharmacology 2006;31:2384–93. 1301165 [pii]\r10.1038/sj.npp.1301165.